

Infrared studies of *ab*-plane oriented oxide superconductors

T. Timusk,* S. L. Herr, K. Kamarás,† C. D. Porter, and D. B. Tanner
Department of Physics, University of Florida, Gainesville, Florida 32611

D. A. Bonn, J. D. Garrett, C. V. Stager, J. E. Greedan, and M. Reedyk
Institute for Materials Research, McMaster University, Hamilton, Ontario, Canada L8S4M1

(Received 14 April 1988)

New results covering a wide frequency and temperature range are presented for the infrared properties of $\text{YBa}_2\text{Cu}_3\text{O}_{7-\delta}$ for light polarized in the *ab* plane. The normal-state optical conductivity can be described by two processes: a low-frequency Drude absorption that tracks the temperature dependence of the dc conductivity and a temperature-independent midinfrared band. In the superconducting state most of the oscillator strength of the Drude absorption moves to zero frequency and the reflectance spectrum is dominated by a plasma edge at 500 cm^{-1} . A superconducting gap cannot be seen in our spectra.

I. INTRODUCTION

The infrared properties of the high-temperature superconductors have attracted considerable attention recently,¹⁻¹⁰ with many attempts to determine the superconducting energy gap as well as some controversy over whether the midinfrared spectrum is a simple Drude absorption centered at zero frequency or a strong midinfrared band. In this paper, we present the results of a detailed study of the temperature dependence of the infrared properties over a wide range of frequencies in *ab*-plane oriented samples of $\text{YBa}_2\text{Cu}_3\text{O}_{7-\delta}$. We find that, averaged over the *ab* plane, the midinfrared region is dominated by a strong, nearly temperature-independent absorption band, possessing around 80% of the infrared oscillator strength. In addition, at temperatures above the superconducting transition temperature, a Drude contribution is observed in the far infrared; the temperature dependence of this Drude term is in agreement with the dc conductivity.

Below T_c , the Drude contribution is not in evidence, suggesting that most of the carriers responsible for the dc transport have condensed to form a collective state. A finite residual absorption remains at low temperatures, possibly the low-frequency tail of the midinfrared band; an energy-gap structure is not discernable in the frequency-dependent conductivity of our samples. Although a peak is seen at 500 cm^{-1} in the superconducting to normal reflectance ratio of crystals, this peak is not the energy gap. Instead, it can be associated with a plasmon-like mode of the superconducting electrons, sufficiently screened by the positive contribution to the dielectric function of the midinfrared absorption band so that it appears in the far infrared.^{1,2}

II. EXPERIMENTAL DETAILS

Our measurements have been made on ceramic samples and on mosaics of small crystals. As we have shown previously,⁸ the as-grown surface of pressed-pellet ceramic samples can have a high degree of orientation, with about

80% of the surface consisting of tilelike crystallites, $10\text{ }\mu\text{m}$ in size, with their *a* and *b* axes lying in the surface. We call these samples "textured" ceramic samples. The crystal mosaic consisted of ten to twenty small flux-grown crystals, each $300\text{--}1500\text{ }\mu\text{m}$ in size. On account of the well-known *ab* twinning which occurs in $\text{YBa}_2\text{Cu}_3\text{O}_{7-\delta}$ crystals, the reflectance of each crystal in the mosaic is an average of the *a*-axis and *b*-axis response.

The crystals were grown from copper oxide rich flux of molar composition $4\text{CuO:1YBa}_2\text{Cu}_3\text{O}_7$ in alumina crucibles. The thermal treatment conditions involved holding at 1065°C for 10 h followed by cooling to 750°C over 60 h. The sample was quenched to 500°C and cooled to 300°C over 40 h. A stream of pure oxygen was bubbled through the charge during all of the above stages.

Typical crystals were thin ($50\text{--}100\text{ }\mu\text{m}$) rectangular plates $1\text{--}2\text{ mm}$ on an edge. Chemical analysis by the neutron activation technique indicated an aluminum content of the crystals of $2\text{--}6\text{ at.}\%$. The T_c for the crystals from the same growth batch measured by the Meissner effect was $85 \pm 2\text{ K}$. This is consistent with published results on aluminum-doped $\text{YBa}_2\text{Cu}_3\text{O}_{7-\delta}$ crystals.¹¹

We measured the far-infrared through near ultraviolet reflectance of our samples between liquid helium and room temperature. Following the measurement, the surfaces of the sample were coated with an ordinary metal (Pb or Al) and the reflectance of the coated surface was measured in order to estimate the amount of incident light lost due to imperfect sample surfaces. Because of the rough surfaces of the textured ceramics and the incomplete parallelism of the crystals making up the mosaic this coating was an extremely important part of the measurement procedure. The frequency-dependent conductivity and dielectric function were determined by a Kramers-Kronig analysis of the reflectance and by least-squares fits to oscillator models.

III. RESULTS

We find two principal contributions to the *ab* plane infrared conductivity of $\text{YBa}_2\text{Cu}_3\text{O}_{7-\delta}$: a Drude part in the

far-infrared and a midinfrared band. In addition, in the textured sample, there is an additional contribution of sharp lines from phonons. These are illustrated in Fig. 1, which shows the 110-K frequency-dependent conductivity of a textured ceramic sample. The smooth curve is the optical conductivity calculated from a fit to the measured reflectance of a dielectric function of the form

$$\epsilon(\omega) = \frac{-\omega_{pD}^2}{\omega^2 + i\omega/\tau} + \sum_{j=1,6} \frac{S_j \omega_j^2}{\omega_j^2 - \omega^2 - i\omega\gamma_j} + \frac{\omega_{pe}^2}{\omega_e^2 - \omega^2 - i\omega\gamma_e} + \epsilon_\infty,$$

where the first term is a Drude contribution characterized by plasma frequency $\omega_{pD} = 5900 \text{ cm}^{-1}$ (0.74 eV) and relaxation rate $1/\tau = 300 \text{ cm}^{-1}$ (0.037 eV); the second is from six optical phonons, with frequencies ω_j , damping constants γ_j , and oscillator strengths S_j ; the third the contribution of the midinfrared absorption band, represented by a highly overdamped oscillator with center frequency $\omega_e = 2100 \text{ cm}^{-1}$ (0.26 eV), strength $\omega_{pe} = 21000 \text{ cm}^{-1}$ (2.6 eV), and width $\gamma_e = 8400 \text{ cm}^{-1}$ (1 eV); the last the high-frequency value of ϵ_1 , here taken to be $\epsilon_\infty = 3.8$. The individual contributions of the far-infrared Drude term and the midinfrared absorption are shown as dashed lines in Fig. 1.

The far-infrared Drude conductivity is consistent with the dc conductivity, both in magnitude and in temperature dependence. Figure 2 shows the frequency-dependent conductivity at three temperatures. With decreasing temperature, the low-frequency (100 cm^{-1}) conductivity increases steadily. In contrast, the midinfrared conductivity shows minimal temperature dependence; most importantly, it does not narrow as it would if there were a single Drude conductivity in the entire infrared range. The inset

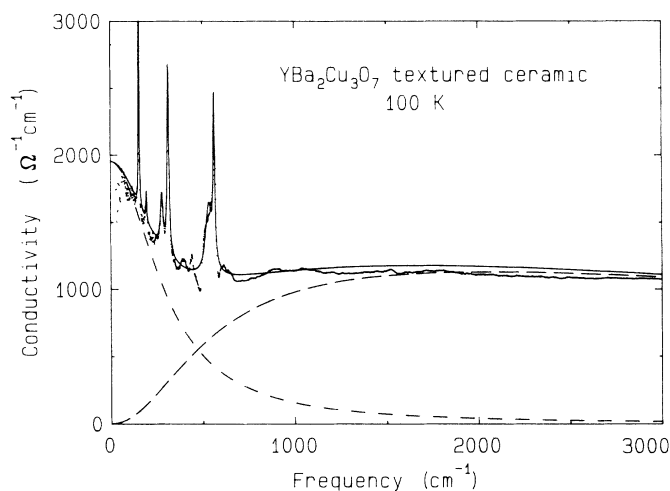


FIG. 1. The optical conductivity of the textured ceramic of $\text{YBa}_2\text{Cu}_3\text{O}_{7-\delta}$ obtained by Kramers-Kronig transformation of the reflectance is shown as points. The smooth curve is a fit of the reflectance to a dielectric function that uses Lorentz oscillators to describe the phonons and a broad band for the midinfrared oscillator strength in addition to a Drude absorption centered on zero frequency. The dashed curves show individual contribution of the Drude and the midinfrared bands to the conductivity.

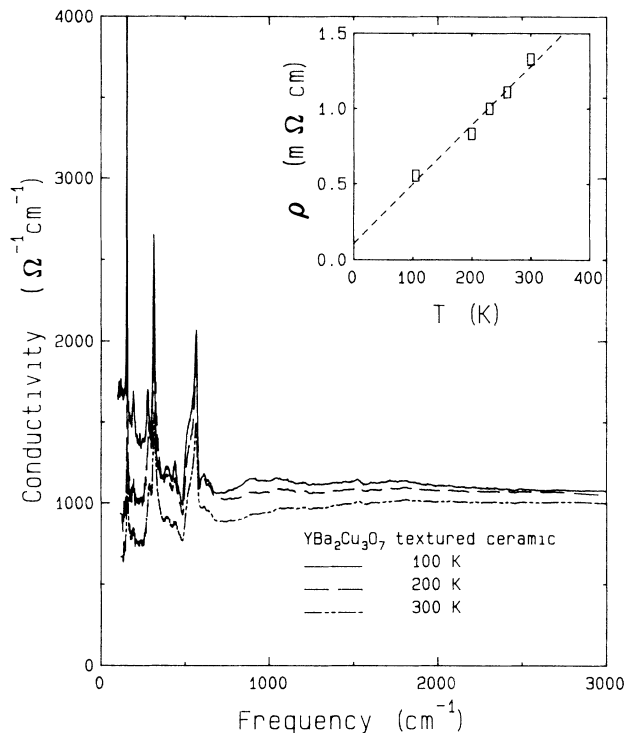


FIG. 2. Temperature dependence of the conductivity. Inset: the resistivity, measured by far-infrared means of 100 cm^{-1} , as a function of temperature. It shows the characteristic linear resistivity of oxide superconductors. The amplitude of the broad mid-infrared band at 2000 cm^{-1} changes little with temperature.

to Fig. 2 gives the temperature dependence of the resistivity ρ measured by far-infrared means; the resistivity is the inverse of the 100-cm^{-1} conductivity. The resistivity is linear in temperature, with a relatively small zero-temperature intercept, typical of high-quality $\text{YBa}_2\text{Cu}_3\text{O}_{7-\delta}$.

The magnitude of the far-infrared resistivity is about 50% larger than the measured dc resistivity for the ceramic sample, a difference which we attribute to a combination of the inaccuracies of the two methods and the fact that the dc measures the entire bulk whereas the far infrared measures only the surface.

Figure 3 shows the reflectance for a single-crystal mosaic at 100 K in the normal state, and at low temperature in the superconducting state. A simple model fit to the normal-state data is also shown: a Drude absorption at zero frequency with $\omega_p = 9700 \text{ cm}^{-1}$ (1.2 eV) and $1/\tau = 250 \text{ cm}^{-1}$ (0.03 eV) and a midinfrared band represented as before with a single broad oscillator. This oscillator has center frequency $\omega_e = 1500 \text{ cm}^{-1}$ (0.19 eV), strength $\omega_{pe} = 20700 \text{ cm}^{-1}$ (2.6 eV), and width $\gamma_e = 3600 \text{ cm}^{-1}$ (0.45 eV). Compared to the parameters which fit the textured sample of Figs. 1 and 2, the crystal mosaic yielded for the midinfrared band a slightly lower frequency and about half the width but essentially identical oscillator strength. Finally, calculations of reflectance which use only a Drude term are also shown in Fig. 3. The higher reflectance curve uses parameters that fit the far

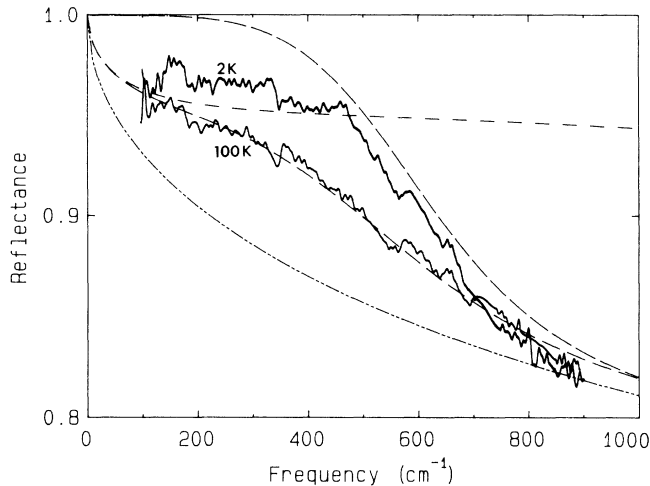


FIG. 3. Reflectance of a single-crystal mosaic of $\text{YBa}_2\text{Cu}_3\text{O}_{7-\delta}$ at 100 K in the normal state and at 2 K in the superconducting state (solid, thick curves). In the superconducting state the reflectance does not reach unity. The shoulder that develops at around 400 cm^{-1} we associate with a plasma edge. The dashed curves show various model fits described in the text: — — —, Drude plus midinfrared oscillator; - - - - -, Drude fit to midinfrared; - · - · -, Drude fit to far infrared; · · · · ·, plasma model for the superconducting state. The best fit to the normal state curve is obtained by assuming a midinfrared band and a low-frequency Drude band. There is no evidence of a superconducting gap in these data.

infrared (given above) while the lower curve fits the midinfrared region with a single Drude expression with $\omega_p = 25000 \text{ cm}^{-1}$ (3.1 eV) and $1/\tau = 4100 \text{ cm}^{-1}$ (0.5 eV). It is clear that a single Drude expression cannot fit the whole curve.

IV. DISCUSSION

A. Normal-state properties

The fit to the reflectance of the crystals shows that 80% of the infrared oscillator strength is in the midinfrared band, with only about 20% in the low-frequency Drude absorption. The total oscillator strength, given by $(\omega_{pD}^2 + \omega_p^2 e) = (2.9 \text{ eV})^2$, is close to what is found by earlier fits to a single Drude model, which found⁷ $\omega_p = 25000 \text{ cm}^{-1}$ (3.1 eV) and $1/\tau = 7500 \text{ cm}^{-1}$ (0.9 eV). The Drude plasma frequency seems to be the most sample-dependent quantity, being some 60% higher in the case of the crystal mosaic than in the textured ceramic, reflecting the higher dc conductivity and greater degree of orientation of the crystals.

We can estimate the mean free path from the relaxation time found in the fit. Using $l = v_F \tau$, and taking $v_F = 2 \times 10^7 \text{ cm/sec}$, our relaxation rate of $1/\tau = 300 \text{ cm}^{-1}$ yields $l = 35 \text{ \AA}$. This is a much more reasonable value than the 1–2 \AA mean free path estimated from the $1/\tau = 4100 \text{ cm}^{-1}$ required to fit the reflectance to a single Drude dielectric function.

B. Superconducting state properties

Because an ordinary superconductor has no loss for photon energies smaller than the energy gap, 2Δ , the reflectance is unity below the gap, and falls to join the (Drude) normal-state reflectance at frequencies substantially above the gap. The ratio of the reflectance in the superconducting state at low temperature to the normal-state reflectance above the superconducting transition temperature, denoted R_s/R_n , has a maximum near 2Δ . Attempts to use measurements of R_s/R_n to determine the superconducting gap in the new high- T_c materials from analogy to ordinary superconductors have been made by many groups,^{6,7,12–15} with estimates of $2\Delta/k_B T_c$ ranging from 1.5 to 8.

The high- T_c materials have a complex dielectric response: it has been shown^{1,2} that in superconducting $\text{La}_{2-x}\text{Sr}_x\text{CuO}_4$ a plasma edge develops in the far infrared. This edge looks deceptively like a BCS gap edge in that it appears in concert with the superconducting transition and that its position and amplitude change with temperature following the BCS order parameter. These changes in reflectance can be traced to the real part of the dielectric function $\epsilon_1(\omega)$, which is large and negative at very low frequencies due to the zero-frequency Δ -function response of the condensed superfluid electrons, but which becomes nearly zero in the far infrared due to the screening of the large positive contribution to $\epsilon_1(\omega)$ from phonons and the midinfrared band. The position of this plasma edge is determined by a balance between the oscillator strengths of the mid-infrared band and the phonons on the one hand and the oscillator strength of the condensate on the other; it does *not* indicate the energy gap.²

Sherwin, Richards, and Zetti¹ have introduced a simple zero-parameter model, the plasmon model, to describe the superconducting state in $\text{La}_{2-x}\text{Sr}_x\text{CuO}_4$. This model assumes that all of the oscillator strength which in the normal state resided in the Drude band of width $1/\tau$ has been shifted to a delta function at zero frequency. The model does not involve any particular value for the gap so long as $2\Delta \gg 1/\tau$.

The dramatic changes seen in the reflectance on passing through the superconducting transition are due to the transfer of most of the oscillator strength of the normal electrons with their Drude response to the zero-frequency delta-function response of the condensate. In the clean limit, the width of the Drude $\sigma_1(\omega)$ is smaller than the gap, making the magnitude of the conductivity at $\omega = 2\Delta$ rather small. In other words, the shoulder at the gap in the Mattis-Bardeen¹⁶ conductivity vanishes in the clean limit. In addition, there remains a finite conductivity from the midinfrared absorption to further diminish the importance of any contribution from the superconducting electrons at and above the gap. Thus there is no sharp feature in the clean-limit reflectance at the gap frequencies; the far-infrared reflectance is determined by the inductive response of the condensate and the reactive and absorptive contribution of the midinfrared band.

The only parameter that can be found from an analysis of infrared data in the clean limit is the temperature dependence of the condensate fraction. Sherwin *et al.*¹ used BCS theory in the weak-coupling limit to calculate

this fraction; however, similar temperature dependences can be found for other models such as gapless superconductivity or boson condensation models. The accuracy of experiments at this stage does not allow a choice among the detailed functional dependence for the various models. Sherwin *et al.* found that not only was it impossible to extract an energy gap from the data, it was not possible to distinguish between the plasmon (clean limit) and energy-gap (dirty limit) response without an *a priori* knowledge of the gap value. In the present work, we have shown that the dirty limit is inappropriate and that the measurements can be explained well by any clean-limit model, independent of the value of the gap.

The dash-dot line in Fig. 3 shows R_s calculated from the plasmon model. The calculation assumes that the superconducting-state dielectric function consists of ϵ_∞ , the midinfrared absorption, and the superconducting-state response. Figure 4 shows the ratio R_s/R_n of the crystal mosaic. The shape of the data is in good agreement with other results⁷ on *ab*-plane crystal surfaces. A band of 2%–4% strength can be seen peaking at 500 cm^{-1} . The plasmon model calculation is also shown. The model describes the position of the peak correctly but it is important to stress that because there remains a low-frequency absorption in our sample, the reflectance does not reach the expected 100% at low frequency.

The plasmon model assumes the extreme clean limit $1/\tau \ll 2\Delta$ for the normal-state conductivity at low temperature. Figure 5 shows the results of a series of calculations of where this assumption is not made. It can be seen that the true gap can only be seen in the dirty limit $\eta \gg 1$ where $\eta = (2\tau\Delta)^{-1}$ while in the clean limit R_s/R_n is dominated by the plasma maximum at 500 cm^{-1} for all values of the gap. We used parameters fitted to the reflectance in the normal state to describe the normal-state properties

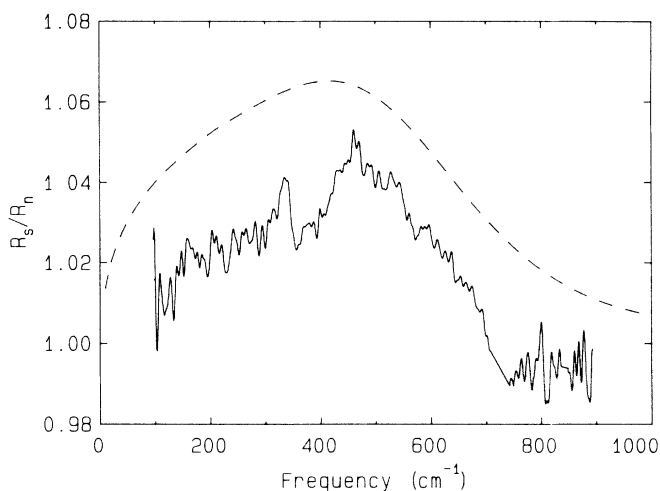


FIG. 4. The ratio of the reflectance in the superconducting state to the reflectance in the normal state at 100 K. This ratio would peak at the energy gap 2Δ in a BCS superconductor. Shown as a dashed line is a calculation that simply assumes that the electrons have condensed to highly conducting state and that the gap is larger than $1/\tau$. The peak is associated with a decrease to nearly zero in the real part of the dielectric function.

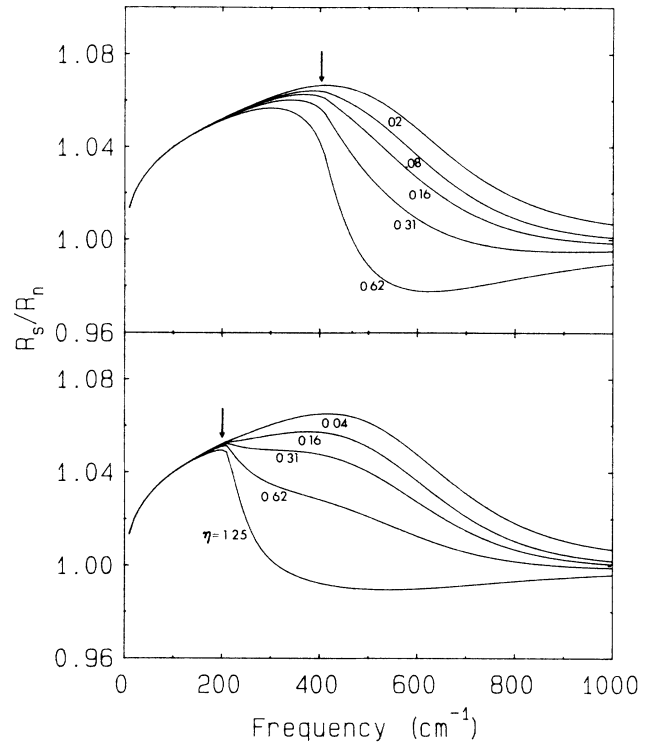


FIG. 5. Calculated reflectance ratio R_s/R_n for a BCS superconductor with $2\Delta/k_B T_c$ of 3.5 (bottom) and 7.0 (top) for various values of $\eta = (2\tau\Delta)^{-1}$. When this parameter is large the superconducting gap, shown as an arrow, can be seen in the reflectance ratio. For $\eta \ll 1$ the plasma maximum dominates the reflectance and the gap cannot be seen. The calculation uses the parameters from the normal-state fit to $\text{YBa}_2\text{Cu}_3\text{O}_{7-\delta}$ shown in Fig. 3.

and the Mattis-Bardeen¹⁶ expression for the superconducting state. The midinfrared oscillator is assumed to be temperature independent and not changed in the superconducting state.

It should be emphasized that the plasma edge seen in the superconducting state at 500 cm^{-1} is a direct consequence of the dispersion caused by the strong midinfrared oscillator strength. Single-crystal R_s/R_n data⁷ show a maximum near 500 cm^{-1} , indicating the plasma model with the same parameters used here can explain those results. No gap value can be inferred from the existing far-infrared data.

C. Midinfrared absorption

The midinfrared absorption has been termed a Drude absorption,^{7–9} but we would like to reserve this term for an absorption that is centered at zero frequency with a constant relaxation time. Physically a Drude absorption corresponds to elastic-scattering processes, typically by impurities or other defects in the crystal such as thermally generated phonons. The zero-frequency limit of the Drude conductivity is the dc resistance. The far-infrared absorption in the *ab*-plane samples, as we have shown, has this Drude behavior.

Is it possible that the midinfrared absorption is the high-frequency portion of another Drude band due to a parallel channel of carriers with a very short temperature-independent relaxation time? We can rule out this notion from the lack of saturation of the dc resistance at high temperature. The overall conductivity of the midinfrared absorption is about $1500 \Omega^{-1}\text{cm}^{-1}$ measured at 1000 cm^{-1} . If this conductivity persisted to zero frequency, the dc conductivity, at high temperature, would be expected to saturate at this value when the temperature-dependent (low-frequency Drude) conductivity became negligible. From the analysis of the high-temperature resistivity of Gurvitch and Fiory¹⁷ one can estimate that the high-temperature saturation conductivity of our sample is less than $300 \Omega^{-1}\text{cm}^{-1}$. Thus, any temperature-independent parallel conductivity channel would have to have a lower conductivity than this. It follows that the midinfrared band is a true inelastic absorption process involving finite energy excitations and not an elastic process centered at zero frequency.

There are several possible mechanisms for this absorption process. On the one hand, it could be due to an interaction between the charge carriers and some excitations such as lattice vibrations, spin fluctuations (spinons), or excitons. In this case, it would be a Holstein sideband of the zero-frequency (Drude) mode. Such a band would always be very broad. At low temperature, the low-energy shoulder is at the average frequency of the scattering excitation; the band peaks at several times this frequency and falls off as $1/\omega^2$ at high frequencies.¹⁸ On the other hand, the absorption could be the result of a direct excitation of a charge degree of freedom such as a charge transfer (exciton) or an interband excitation. The great width of the band is not inconsistent with the exciton picture, as one would not expect to see narrow hydrogenic exciton lines in strongly correlated systems.

The midinfrared band is not unique to $\text{YBa}_2\text{Cu}_3\text{O}_{7-\delta}$

but has been observed in all the oxide superconductors. In $\text{La}_{2-x}\text{Sr}_x\text{CuO}_4$ (Refs. 4 and 19–21) ceramics it has been shown to follow the dopant Sr concentration closely, although the shape of the band in ceramics is heavily distorted by the random orientation of the highly anisotropic grains, as pointed out by Orenstein and Rapkine.²² Similarly, in $\text{BaPb}_{1-x}\text{Bi}_x\text{O}_3$, there is a non-Drude absorption at 2000 cm^{-1} of $\approx 2000 \Omega^{-1}\text{cm}^{-1}$ strength that appears only for x values that result in superconductivity.²³ The earliest of the perovskite superconductor discovered, doped SrTiO_3 , also shows a well-defined non-Drude peak²⁴ centered at 2000 cm^{-1} . The last two examples are single-crystal measurements in cubic crystal structures without any interference from anisotropy complicated by *ab*-plane domain disorder. In these cases the peak seems to be better defined than in our results here. Recent important results²⁵ on single-domain $\text{YBa}_2\text{Cu}_3\text{O}_{7-\delta}$ crystals also show a well-defined conductivity peak polarized mainly in the *b* direction at 2500 cm^{-1} (0.3 eV). This strong anisotropy is an indication that the optical response that gives rise to the midinfrared peak in $\text{YBa}_2\text{Cu}_3\text{O}_{7-\delta}$ is not confined to the copper-oxygen planes and that an excitonic coupling to atoms not in this plane may well be important in high-temperature superconductivity.

ACKNOWLEDGMENTS

Z. Bazinski, H. F. Gibbs, M. A. Crowe, and A. Pie-druczny contributed to the crystal-growth and characterization experiments. This research was supported at McMaster by the Natural Science and Engineering Research Council of Canada (NSERC), including infrastructure support for the Institute for Materials Research and the McMaster Nuclear Reactor and in Florida by National Science Foundation Grant No. DMR-8416511. One of us (T.T.) would like to thank the University of Florida for generous hospitality and support.

*Permanent address: Department of Physics, McMaster University, Hamilton, Ontario, Canada L8S4M1.

†Permanent address: Central Research Institute for Physics, P. O. Box 49, H-1525 Budapest, Hungary.

¹M. S. Sherwin, P. L. Richards, and A. Zettl, *Phys. Rev. B* **37**, 1587 (1988).

²D. A. Bonn, J. E. Greedan, C. V. Stager, T. Timusk, M. G. Doss, S. L. Herr, K. Kamarás, C. D. Porter, and D. B. Tanner, *Phys. Rev. B* **35**, 8843 (1987).

³D. A. Bonn, A. H. O'Reilly, J. E. Greedan, C. V. Stager, T. Timusk, K. Kamarás, and D. B. Tanner, *Phys. Rev. B* **37**, 1547 (1988).

⁴J. Orenstein, G. A. Thomas, D. H. Rapkine, C. B. Bethea, B. F. Levine, B. Batlogg, R. J. Cava, and D. W. Johnson, Jr., *Phys. Rev. B* **36**, 8892 (1987).

⁵S. Sugai, *Phys. Rev. B* **36**, 7133 (1987).

⁶A. Wittlin, L. Genzel, M. Cardona, M. Bauer, W. König, E. Garcia, M. Barahona, and M. V. Cabañas, *Phys. Rev. B* **37**, 652 (1988).

⁷Z. Schlesinger, R. T. Collins, D. L. Kaiser, and F. Holzberg, *Phys. Rev. Lett.* **59**, 1958 (1977); R. T. Collins, Z. Schles-

inger, R. H. Koch, R. B. Laibowitz, T. S. Plaskett, P. Freitas, W. J. Gallagher, R. L. Sandstrom, and T. R. Dinger, *ibid.* **59**, 704 (1978); Z. Schlesinger, R. T. Collins, M. W. Shafer, and E. M. Engler, *Phys. Rev. B* **36**, 5275 (1987).

⁸I. Bozovic, D. Kirilov, A. Kapitulnik, K. Char, M. R. Hahn, M. R. Beasley, T. H. Geballe, Y. H. Kim, and A. J. Heeger, *Phys. Rev. Lett.* **59**, 2219 (1987).

⁹S. Tajima *et al.* (unpublished).

¹⁰T. W. Noh, P. E. Sulewski, and A. J. Sievers, *Phys. Rev. B* **36**, 8866 (1987).

¹¹T. Siegrist, L. F. Schneemeyer, J. V. Waszczak, N. P. Singh, R. L. Opila, B. Batlogg, L. W. Rupp, and D. W. Murphy, *Phys. Rev. B* **36**, 8365 (1987).

¹²U. Walter, M. S. Sherwin, A. Stacy, P. L. Richards, and A. Zettl, *Phys. Rev. B* **35**, 5327 (1987).

¹³P. E. Sulewski, A. J. Sievers, S. E. Russek, H. D. Hallen, D. K. Lathrop, and R. A. Buhrman, *Phys. Rev. B* **35**, 5330 (1987).

¹⁴Z. Schlesinger, R. T. Collins, and M. W. Schafer, *Phys. Rev. B* **35**, 7332 (1987).

¹⁵D. A. Bonn, J. E. Greedan, C. V. Stager, and T. Timusk, *Solid*

- State Commun. **62**, 838 (1987).
- ¹⁶D. C. Mattis and J. Bardeen, Phys. Rev. **111**, 412 (1958).
- ¹⁷M. Gurvitch and A. T. Fiory, Phys. Rev. Lett. **59**, 1337 (1987).
- ¹⁸P. B. Allen, Phys. Rev. B **3**, 305 (1971).
- ¹⁹S. L. Herr, K. Kamarás, C. D. Porter, M. G. Doss, D. B. Tanner, D. A. Bonn, J. E. Greedan, C. V. Stager, and T. Timusk, Phys. Rev. B **36**, 733 (1978).
- ²⁰S. Etamad, D. E. Aspnes, M. K. Kelly, R. Thompson, J.-M. Tarascon, and G. W. Hull, Phys. Rev. B **37**, 3396 (1988).
- ²¹S. L. Herr *et al.*, in *High Temperature Superconducting Materials: Preparations, Properties and Processing*, edited by William Hatfield and J. J. Miller (Marcel Dekker, New York, 1988), p. 275.
- ²²Joseph Orenstein and D. H. Rapkine, Phys. Rev. Lett. **60**, 968 (1988).
- ²³S. Tajima, J. Uchida, A. Maski, H. Tagaki, K. Kitizawa, and S. Tanaka, Phys. Rev. B **32**, 6302 (1985).
- ²⁴A. S. Barker, in *Optical Properties and Electronic Structure of Metals and Alloys*, edited by F. Abelés (North-Holland, Amsterdam, 1965).
- ²⁵J. Tanaka, K. Kama, M. Shimizu, M. Simada, C. Tanaka, H. Ozeki, K. Adachi, K. Iwahashi, F. Sato, A. Sawada, S. Iwata, H. Sakuma, and S. Uchiyama, in *Proceedings of International Conference on High Temperature Superconductors: Materials and Mechanisms of Superconductivity, Interlaken, 1988* [Physica C **153–155**, 1752 (1988)].